Radiation-induced fragmentation of fullerenes

Titus A. Beu* and Aurel Jurjiu
Faculty of Physics, University "Babeş-Bolyai," 400084 Cluj-Napoca, Romania
(Received 12 September 2010; published 25 January 2011)

The radiation-induced fragmentation of the fullerenes C_{36}, C_{60}, C_{70}, and C_{96} was investigated by tight-binding molecular dynamics simulations. The resulting fragment size and fragment charge distributions, averaged over large ensembles of trajectories corresponding to total ionization states up to $+20e$ and excitation energies up to 300 eV, have been used to analyze the fragmentation statistics in terms of several derived quantities. A well-defined phase transition region is found in the total charge-excitation energy plane, which appears to be delimited by critical lines depending quadratically on the total ionization charge and linearly on the fullerene size.

DOI: 10.1103/PhysRevB.83.024103 PACS number(s): 71.20.Tx, 36.40.Qv, 61.48.−c, 31.15.aq

I. INTRODUCTION

Twenty-five years after their discovery, fullerenes continue to attract considerable interest due to their exceptional properties and yet emerging applications. Fullerenes can undergo a wide variety of processes ranging from charge transfer and ionization to atom capture, fusion, and fragmentation.[1,2] Despite the presently available high-yield production methods (based on combustion synthesis and arc discharges), the very mechanisms of fullerene formation are only partially understood. From a reverse perspective, besides its intrinsic importance, fullerene fragmentation is also capable of offering insight into the formation process.

The majority of C_{60} fragmentation experiments, independent of the specific excitation mechanism, evidence typically *charged* fragments,[3–5] a significant detail which adds to the complexity and is often disregarded in calculations. By contrast, the neglect of the electron-phonon coupling appears to be less important due to the short energy-deposition times found in experiments.[6]

Our initial tight-binding (TB) molecular dynamics studies concerning the fragmentation of C_{60},[7] relying on adiabatic excitation and neglecting the ionization processes, have evidenced a phase transition marked by an abrupt rise in the fragmentation probability at a critical excitation energy of about 100 eV. Subsequently, we have devised more realistic models for the nonadiabatic fullerene excitation and for the ionization and charge-transfer processes induced by femtosecond laser pulses, which have been employed in a comprehensive analysis of the C_{60} fragmentation (Ref. 8, hitherto referred to as paper I). For moderate excitation energies, the fragment size profiles have been found to reproduce the experimentally observed U shape and bimodal dependences.[3]

One of the main findings of our simulations was the existence of a phase transition region in the total charge-excitation energy plane, featuring a critical excitation energy around 90 eV for neutral C_{60} cages and decreasing roughly parabolically with increasing total ionization charge. The charge-averaged critical excitation energy (55 eV) agrees fairly well with the experimental findings of Rentenier *et al.*,[3] but could not possibly have been reproduced if charged fragments were neglected.

The recent semiclassical dynamics simulations of Li *et al.*[9] deal with the photofragmentation of the C_{60} fullerene induced by ultrafast laser pulses. The state of the valence electrons is obtained from the time-dependent Schrödinger equation, while the radiation field and the motion of the nuclei are treated classically. Considering only neutral fragments and relatively small statistical ensembles, Li *et al.* found, in qualitative agreement with our results, that fragmentation follows a bimodal pattern for small pulse intensities, while the distribution of the smaller neutral fragments at high excitation energies follows power laws peaking for C_2 or C_3.

More recently, Hussien *et al.*[10] adopted the concept of the phase transition in a study of the fragmentation and formation of C_{60} and C_{240} as a reverse processes in the vicinity of the critical temperature. A simplified picture was considered, in which single fullerenes decay (recombine) preferentially into (from) neutral C_2 units, while charged species are neglected. The employed "topologically constrained force field," constructed from pairwise Lennard-Jones interactions for predefined lists of atoms, produces distributions that do not show the experimental U shape, exhibiting for moderate excitation energies only isolated C_2 peaks in the small-fragment domain. Furthermore, the larger fullerene C_{240} is reported to have a lower phase transition temperature than C_{60}, while we essentially find a proportional dependence of the critical excitation energy on the fullerene size.

The present paper broadens the scope of our previous work[7,8] and, based on the models already validated in paper I, extends the discussion of the fragmentation statistics from C_{60} to C_{36}, C_{70}, and C_{96}. Starting from the fragment size and fragment charge distributions, as primary results, the dependence of various average synthetic quantities (fragmentation probability, number of fragments, fragment size, number of bonds) on the excitation energy, the total ionization charge, and the fullerene size is discussed. The phase transition we have previously reported is given an additional dimension, namely, the fullerene size, and a model of extreme simplicity for the dependence of the critical excitation energy on the fullerene size and the total ionization charge is proposed.

II. SIMULATION DETAILS

Over more than a decade, we have successfully employed the nonorthogonal TB parametrization of Papaconstantopoulos *et al.*[11] (which can be regarded as a simplified two-center-oriented first-principles method) in

structural and vibrational studies concerning polymers of a variety of fullerenes (C_{36}, C_{60}, and C_{70}),[12–15] and, more recently, in the aforementioned investigations of the C_{60} fragmentation.[7,8] The TB formulation, along with other models and methods employed in the present study, has been described in detail in our previous papers. Yet, a brief review will be given in the following.

As a preparatory step, the equilibrium geometries of the considered fullerene species (C_{36}, C_{60}, C_{70}, and C_{90}) have been optimized with respect to the employed TB force field by simulated annealing and remarkably well-grouped corresponding binding energies per atom have resulted (9.748, 10.023, 10.059, and 10.086 eV).

Our simulations operate with ionized fragments and explicit models for excitation and charge redistribution. The excitation of the fullerenes is accomplished by a ramplike input of kinetic energy and charge over an interval of 0.1 ps. Concretely, at each time step the system acquires equal kinetic energy increments, involving small random corrections of the atomic velocities, which sum up to the desired total excitation energy. In an analogous mechanism for ionization, elementary charges are added at equal time subintervals, yielding the desired total charge at the end of the excitation interval. If the fragmentation occurs during excitation, the charge increment is assigned randomly to one of the produced fragments.

As part of our charge-redistribution model, even though the charge of any fragment is inherently kept integer, the composing atoms can have at times fractional charges. At each time step, any newly formed fragment is assigned at first the sum of the partial charges carried by the atoms composing the originating fragments. The excess fractional charges are then removed from the new fragments (rounding their charges down) and redistributed as integers until exhaustion in increasing order of the initial charge deficit to the next higher integer exhibited by the fragments. By this redistribution scheme, the total ionization state is conserved and the fluctuations in the fragment charges are minimized.

Fragmentation trajectories for total ionization charges up to $+20e$ and excitation energies up to 300 eV (approximately half the total binding energy of C_{60}) have been simulated. For each individual fullerene species and each given combination of total charge and excitation energy, an ensemble of 200 randomly prepared initial configurations have been fragmented and subsequent ensemble statistics has been carried out. Each fragmentation trajectory is propagated using the velocity Verlet algorithm with a constant time step, which depends, however, exponentially on the particular excitation energy, i.e., decreasing from 0.5 fs for 100 eV to 0.05 fs for 500 eV. The fragments are identified by a recursive labeling algorithm.

The termination of any trajectory is triggered when two simultaneous criteria are met—if the fragment size distribution remains unchanged between two consecutive checkpoints (typically, 1000 time steps apart) and if the distance between any two fragments is larger than the extent of the tight-binding C-C potential well (∼4 Å).

III. RESULTS AND DISCUSSION

The fundamental quantities produced in our simulations are the fragment size and the fragment charge distributions.

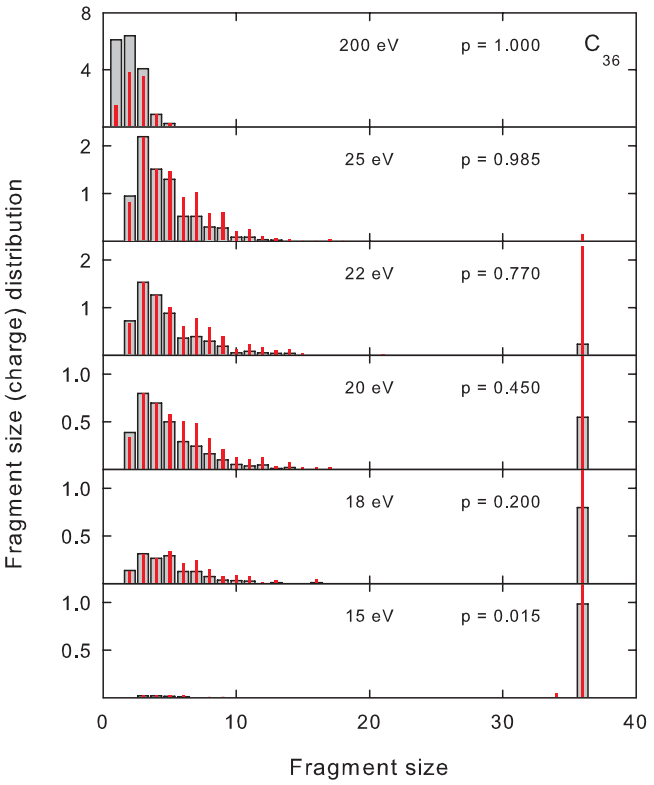

FIG. 1. (Color online) Ensemble-averaged fragment size distributions and fragment charge distributions (as red vertical lines) of C_{36} with a total ionization charge $+10e$ for selected excitation energies (p designates the corresponding fragmentation probabilities).

They are recorded for each combination of total charge and excitation energy as ensemble-averaged distributions and all other quantities of interest are extracted therefrom. As illustrative examples, Figs. 1–3 show the superimposed fragment size and charge distributions of the fullerenes C_{36}, C_{70}, and C_{96} for the total ionization charge $q_{\text{tot}} = 10e$ and for selected ranges of excitation energies. Similar profiles for C_{60} have been presented and discussed at length in paper I.

Despite the different excitation ranges displayed for the different fullerene species, many general features can be discerned, such as, for instance, the gradual shift of the distribution maxima toward smaller fragment sizes with increasing excitation energy and/or total charge. Overall, the size distribution patterns appear to be similar to those from a wide variety of fragmentation experiments with atomic projectiles.[3,16–19]

The average fragmentation probability, providing the most synthetic description of the overall features of the fragmentation process, is defined for each trajectory ensemble as the ratio of the number of dissociative trajectories to the total number of trajectories. The excitation energies corresponding to the lowest panels of Figs. 1–3 mark roughly, as the small but nonvanishing probabilities indicate, the transition from a *fragmentationless* to a *fragmentation regime*, characterized by a strong dependence of the fragmentation probability on the excitation energy. For the total ionization charge used for illustration ($10e$), the fragmentation thresholds can be identified around 15, 60, 80, and 110 eV, respectively, for

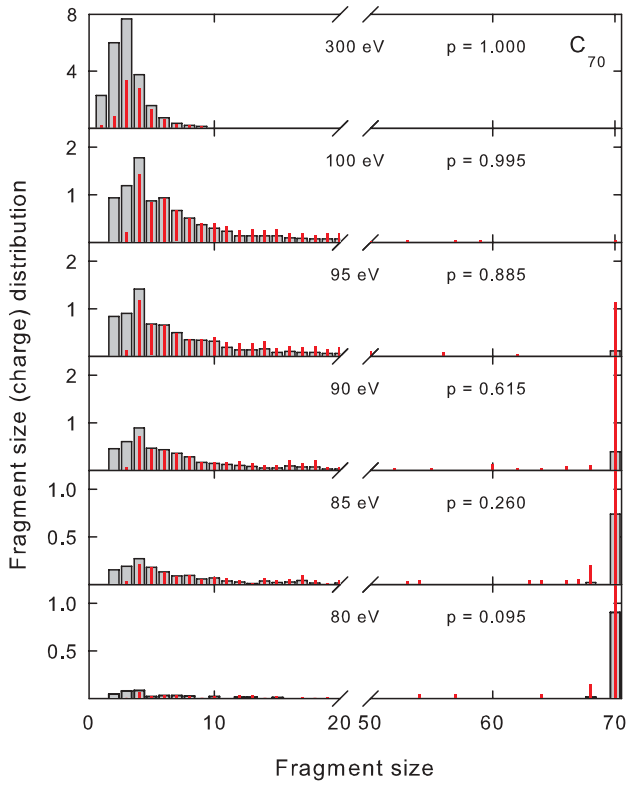

FIG. 2. (Color online) Ensemble-averaged fragment size distributions and fragment charge distributions (as red vertical lines) of C_{70} with a total ionization charge $+10e$ for selected excitation energies (p designates the corresponding fragmentation probabilities).

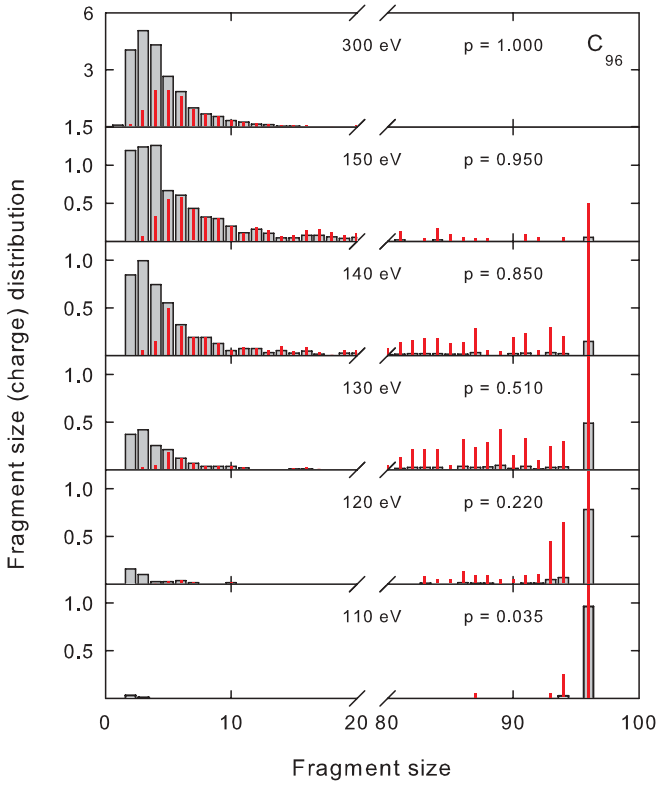

FIG. 3. (Color online) Ensemble-averaged fragment size distributions and fragment charge distributions (as red vertical lines) of C_{96} with a total ionization charge $+10e$ for selected excitation energies (p designates the corresponding fragmentation probabilities).

C_{36}, C_{60}, C_{70}, and C_{96}. As counterparts, the uppermost panels mark the passage to a *saturation regime*, characterized by unitary fragmentation probability (every single trajectory leads to fragmentation of the fullerene cage).

U-shaped size distributions (with absent C monomers) have been evidenced experimentally among others by Rentenier *et al.*[3] and can be identified for the total ionization charge under consideration only in the case of the larger C_{96} (up to about 130 eV), since C_{96}, in particular, carries the smallest specific ionization charge ($q_{\mathrm{tot}}^2/N_{\mathrm{atom}} \sim 1e^2/\mathrm{atom}$) and is thus subject to moderate electrostatic interactions. The smaller fullerenes no longer show U-shaped distributions due to the stronger Coulomb repulsion per atom, which leads to the successive disintegration of large fragments into smaller ones. In fact, the limiting total ionization charge

$$q_{\mathrm{U}} = \sqrt{N_{\mathrm{atom}}} \tag{1}$$

still leading to U-shaped fragmentation profiles proves to apply to all fullerene species. Furthermore, a bimodal size dependence appears to characterize predominantly the large fragments, in agreement with other calculations from the literature.[20,21]

The upper panels of Figs. 1–3 prefigure the transition to power laws, which become obvious for energies above 1000 eV. The excitation energy being on average equally distributed between translational and rotational degrees of freedom, roughly twice the molecular binding energy (~700 eV for C_{36} to ~2000 eV for C_{96}) would be required to fully dissociate the neutral fullerenes. However, our simulations show that even for higher excitation energies, due to the substantial kinetic energy acquired by the fragments, besides monomers, albeit rarely, carbon dimers still remain discernible at the end of the trajectories.

The average charge distributions, specifying the average charge accumulated by *all* fragments of a given size, apparently behave similarly to the fragment size distributions (Figs. 1–3). Nevertheless, a certain lag of the charge on the larger fragments develops with increasing excitation energy and increases with fullerene size. In other words, the smaller the total ionization charge per atom, the more are the charge profiles shifted toward larger sizes. For C_{36}, the charge profiles follow closely the size profiles, since the optimal arrangement for the appreciable specific charge carried in this case is the proportional distribution. On the other hand, a moderate total charge is preferentially accommodated by larger fragments, which reduce the electrostatic repulsion. Indeed, for fragmentation probabilities $p \lesssim 0.5$, the few large fragments stemming from C_{96} can be seen to carry significantly higher charges than the smaller ones.

Figure 4 shows comparatively the fragmentation probability profiles of the four fullerene species as functions of the excitation energy for five illustrative total ionization charges ($q_{\mathrm{tot}} = 0,5e,10e,15e,20e$). Between the fragmentationless low-energy region ($p = 0$) and the plateau corresponding to certain fragmentation ($p = 1$) a well-defined transition region with a monotonic slope is present. The slopes increase and shift

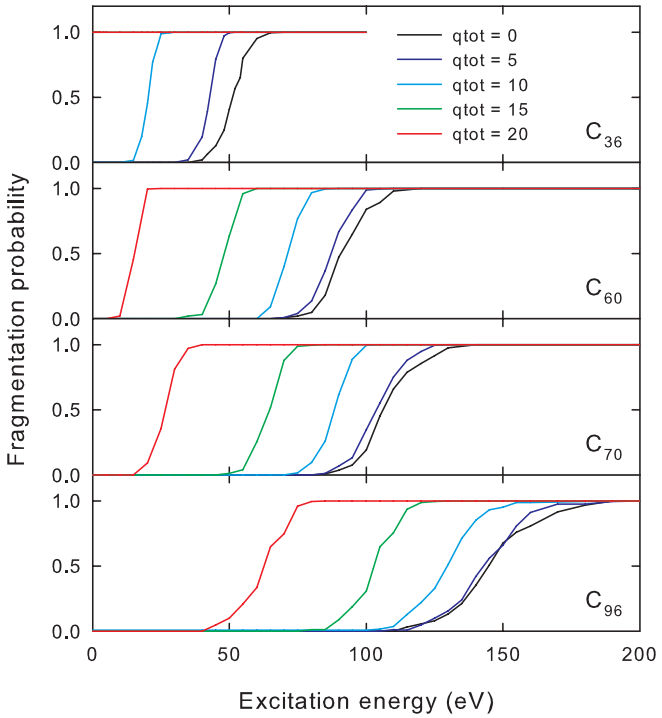

FIG. 4. (Color online) Fragmentation probability profiles for selected total ionization charges as functions of the excitation energy.

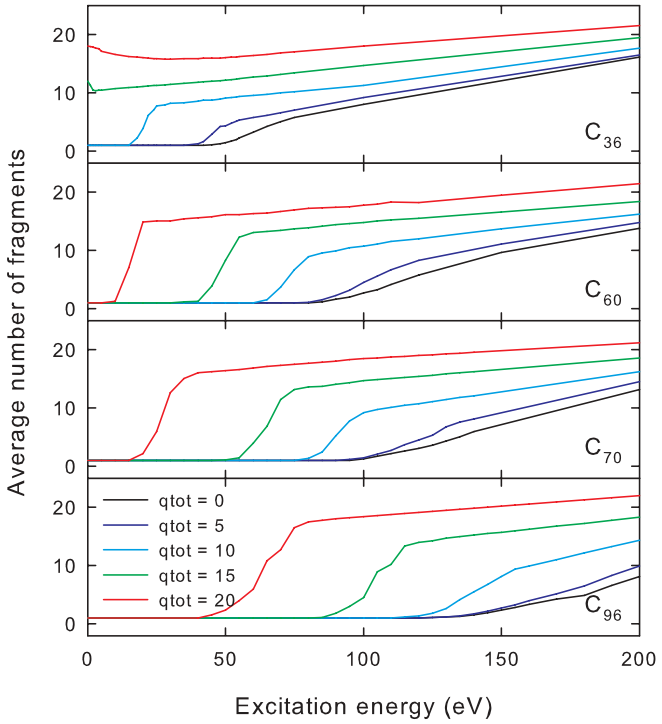

FIG. 5. (Color online) Average number of fragments for selected total ionization charges as functions of the excitation energy.

toward lower excitations with increasing ionization charge, as fragmentation becomes more probable with additional charge input.

As a fundamental synthetic quantity, we define the critical excitation energy for a given total charge as the input energy corresponding to the average fragmentation probability 0.5 (when half of the trajectories lead to fragmentation). The critical energies for the chargeless fragmentation of C_{36}, C_{60}, C_{70}, and C_{96} extracted from the profiles of Fig. 4 are, respectively, 51.2, 90.9, 106.2, and 144.8 eV. The value for C_{60} agrees with earlier simulations of Kim *et al.*[22,23] As will be discussed below, the critical excitation energy decreases roughly quadratically with increasing total ionization state, such that a total charge is eventually reached for which the fragmentation occurs without any energy input. Notably, for C_{36} the total charge $20e$ results in 100% fragmentation.

With the sole exception of C_{36} in the case of the total ionization charge $20e$, the profiles of the average number of fragments as functions of the excitation energy (Fig. 5) can be seen to increase monotonically. In the transition region, the slopes increase considerably with the total charge, indicating high instabilities within the system. In the higher-energy region, the average number of fragments appears to depend roughly linearly on the excitation energy and quadratically on the total ionization state. Obviously, the profiles for each given fullerene species converge asymptotically to the corresponding total number of atoms.

The initial decrease in the particular case of C_{36} with total ionization charge $20e$ is due to the fact that for the small kinetic energies acquired by the fragments in the excitation energy range up to 20–30 eV, the tight-binding contributions can compensate the Coulomb repulsion, such that, instead of a large number of small chainlike fragments, a smaller number of more compact fragments (with increased atomic coordination) are formed. This particular behavior is reflected also in the initial increase in the corresponding plot of the average number of bonds (Fig. 7).

Another illustrative quantity provided by the simulations is the average fragment size (Fig. 6), calculated for each combination of total charge and excitation energy as the average of the ensemble-averaged fragment size distribution. From the total number of atoms in the fragmentationless region, it decreases abruptly in the transition region toward small values with respect to both parameters, tending asymptotically to the limiting value 1 (total fragmentation). The average fragment size is complementary to the average number of fragments and their product remains constant within statistical errors and equal to the total number of atoms.

The fragment compactness may be expressed in terms of the average number of bonds formed by the fragments (Fig. 7). For low-energy nonfragmenting trajectories, for which the fullerene cages are not distorted excessively, the number of bonds of the initial equilibrium structures is preserved. However, bonds start breaking (but also rebuilding) already for excitation energies below the fragmentation threshold. The decrease of the number of bonds is more pronounced with increasing total charge than with increasing excitation energy. For the higher ionization states, the decrease is rather abrupt and roughly monotonic. By contrast, for neutral and low-charge fullerenes a discrete minimum followed by a maximum are noticeable in the transition region, indicating that during and immediately after the initial disintegration, fragments can recombine to a certain extent, producing incidentally compact structures. This leads to an increased average number of

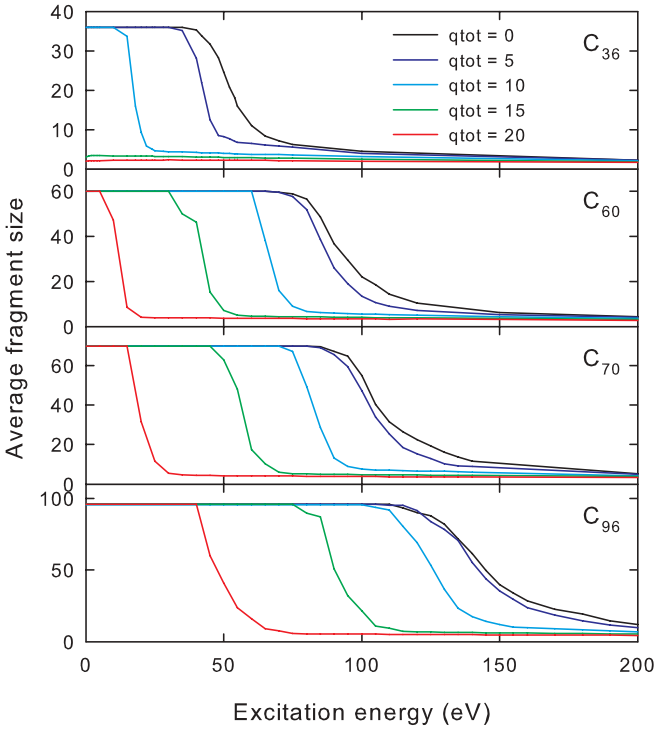

FIG. 6. (Color online) Average fragment size for selected total ionization charges as functions of the excitation energy.

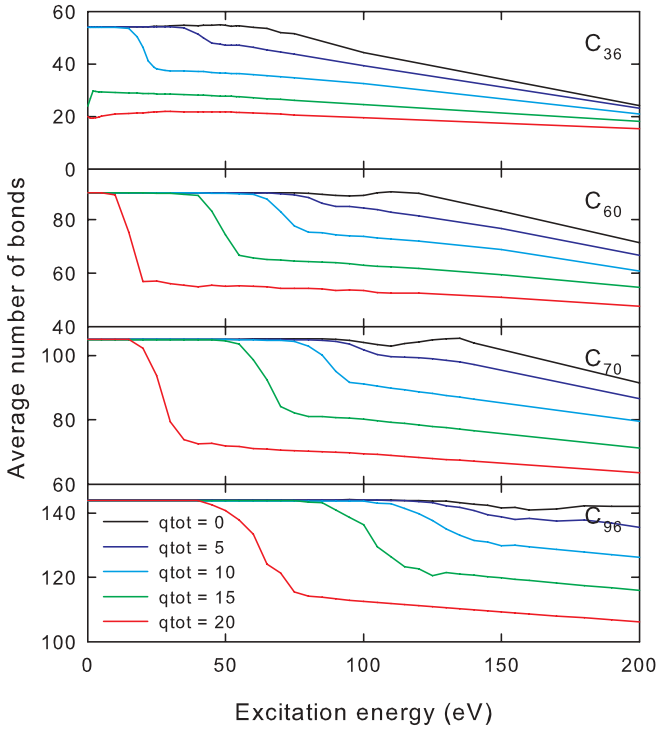

FIG. 7. (Color online) Average number of bonds for selected total ionization charges as functions of the excitation energy.

bonds, sometimes even exceeding the initial one. If sufficient excitation or electrostatic energy is transferred to the system, fragments become less compact and the number of bonds decreases significantly as dissociation progresses.

It is instructive to analyze the fragmentation process in the phase transition region. The critical points for all of the considered fullerenes (Fig. 8) can be fairly well fitted by a surprisingly simple model, which is linear in the fullerene size (initial number of bonds) and parabolic in the total ionization charge:

$$E_{\mathrm{crit}} = aN_{\mathrm{bond}} - bq_{\mathrm{tot}}^2, \tag{2}$$

where the initial number of bonds for all the considered fullerenes is related to the number of atoms simply by $N_{\mathrm{bond}} = 1.5N_{\mathrm{atom}}$. The parameter a is rather a dimensional factor, taking invariably the constant value $a = 1$ eV. The only variable parameter is b, which equals 0.33 eV for C_{36} and 0.2 eV for the rest of the fullerenes. This model basically implies that for *neutral* fullerenes the fragmentation probability 0.5 can be achieved by providing an excitation energy of roughly 1 eV to each bond of the equilibrium configuration. A slightly more accurate and "physical" model is

$$E_{\mathrm{crit}} = 0.15N_{\mathrm{atom}}E_{\mathrm{bind}}^0 - bq_{\mathrm{tot}}^2 \tag{3}$$

and the correspondence with Eq. (2) can be easily understood given $E_{\mathrm{bind}}^0 \simeq 10$ eV for all considered fullerene species.

From an experimental point of view, an estimate of the average critical energy for all ionization states is of considerable interest. Based on the simple assumption that different total charge states occur with equal probability, we found for C_{60} in paper I, by averaging the critical excitation energy over all intermediate integer ionization charges, an approximate value of 55 eV, in fair agreement with the threshold for asymmetric dissociation found by Rentenier *et al.*[3] around 50 eV in fragmentation experiments with $H_{x=1,3}^+$.

By numerically averaging along their critical line, similar results can be obtained for the other fullerene species, as well. However, by considering the model Eq. (2) one can obtain a useful and general rule of thumb for the average critical excitation energy. By defining the critical charge as the charge for which the critical state (fragmentation probability 0.5)

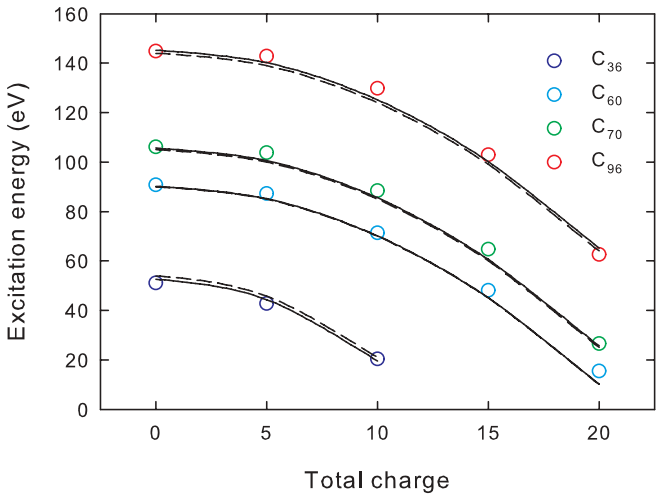

FIG. 8. (Color online) Critical points for selected combinations of excitation energies and total ionization charges and excitation lines based on Eq. (2) (dashed) and Eq. (3) (continuous).

occurs without excitation energy supply,

$$q_{\rm crit} = \sqrt{(a/b)N_{\rm bond}}, \tag{4}$$

and averaging Eq. (2) over all integer charges up to $\overline{q}_{\rm crit} = \lfloor q_{\rm crit} \rfloor$ (as concrete values, $12e$, $21e$, $22e$, and $26e$ for the considered fullerene species), one obtains

$$\langle E_{\rm crit} \rangle = aN_{\rm bond} - \frac{b}{6}(2\overline{q}_{\rm crit} + 1)(\overline{q}_{\rm crit} + 1). \tag{5}$$

Now, by approximating $\overline{q}^2_{\rm crit} \simeq q^2_{\rm crit}$ and using definition Eq. (4), some simple algebra leads to the linear dependence of the average critical energy on the fullerene size:

$$\langle E_{\rm crit} \rangle \simeq aN_{\rm atom} - b\overline{q}_{\rm crit}/2. \tag{6}$$

The correction amounts to values between 2.0 and 2.6 eV, yielding in the case of C_{60} $\langle E_{\rm crit} \rangle \simeq 57.9$ eV (as compared to 55 eV, found by numerical averaging along the whole critical line in paper I). The estimates for C_{36}, C_{70}, and C_{96} given by Eq. (6) are, respectively, 34.0, 67.8, and 93.4 eV. Interestingly, taking rather the *continuous* than the discrete average along the critical line yields $\langle E_{\rm crit} \rangle = aN_{\rm atom}$, i.e., an exactly proportional dependence of the average critical energy on the fullerene size.

IV. CONCLUSIONS

The paper presents a detailed molecular dynamics study of the radiation-induced fragmentation of the C_{60}, C_{36}, C_{70}, and C_{96} fullerenes. The calculations are based on the nonorthogonal tight-binding parametrization of Papaconstantopoulos *et al.*[11] and account explicitly for the nonadiabatic excitation of the fullerenes and the charge-transfer processes undergone by the resulting fragments.

The fundamental quantities yielded by the simulations are the fragment size and fragment charge distributions, averaged over large ensembles of trajectories for given combinations of total ionization states and excitation energies. The fragment size and charge distributions follow similar patterns, shifting toward smaller sizes with increasing energy and/or charge input, but with a manifest tendency of *moderate* total ionization charges to distribute rather on larger fragments. The lag of the charge distributions disappears with increasing specific ionization charge, and the size and charge distributions become proportional. The shift of the charge profiles with respect to the density profiles implies a higher probability of occurrence of small *neutral* fragments (mainly C_2, by successive evaporations). For higher total ionization states and/or excitation energies, we find that the $C_3{}^{q+}$ loss is the dominant channel in agreement with the results of Boyle *et al.*[24] While for low energies, evaporation and cleavage of smaller clusters is the prevailing mechanism, for high excitation energies multifragmentation appears to be the main fragmentation channel. However, genuine power-law distributions become established only beyond 1000 eV, predominantly monomers and dimers being observed for high excitation energies.

For moderate excitation energies and/or total ionization states, the fragment size profiles exhibit the experimentally observed U shape, as well as a bimodal dependence.[1,3,18,19] Nevertheless, irrespective of the excitation energy, in highly ionized states the U-shaped size distributions disappear, since the strong electrostatic repulsion between and within clusters produces further disintegration into smaller fragments. A simple square root dependence on the fullerene size of the limiting ionization charge still producing U-shaped distributions has been found to hold for all studied fullerene species.

Clearly delimited phase transition regions have been identified in the excitation energy dependences of the fragmentation probability for all fullerene species, which separate fragmentationless regions from saturation plateaus. The critical points appear to depend to a fair approximation on the squares of the total ionization charge and linearly on the size for all considered fullerene species. Moreover, the charge-averaged critical excitation energies estimated from the parabolic models have been found to depend linearly on the fullerene size.

ACKNOWLEDGEMENT

This work was supported by CNCSIS-UEFISCSU, Project No. PNII-ID 506/2007.

*titus.beu@phys.ubbcluj.ro

[1] E. B. Campbell and F. Rohmund, Rep. Prog. Phys. **63**, 1061 (2000).
[2] V. V. Afrosimov, A. A. Basalaev, M. N. Panov, and O. V. Smirnov, Fullerenes, Nanotubes, Carbon Nanostructures **12**, 485 (2004).
[3] A. Rentenier, P. Moretto-Capelle, D. Bordenave-Montesquieu, and A. Bordenave-Montesquieu, J. Phys. B **38**, 789 (2005).
[4] I. Shchatsinin, T. Laarmann, G. Stibenz, G. Steinmeyer, A. Stalmashonak, N. Zhavoronkov, C. P. Schulz, and I. V. Hertelb, J. Chem. Phys. **125**, 194320 (2006).
[5] T. Kobayashi, T. Kato, Y. Matsuo, M. Kurata-Nishimura, J. Kawai, and Y. Hayashizaki, J. Chem. Phys. **126**, 061101 (2007).
[6] K. Hansen, K. Hoffmann, and E. E. B. Campbell, J. Chem. Phys. **119**, 2513 (2003).
[7] L. Horváth and T. A. Beu, Phys. Rev. B **77**, 075102 (2008).
[8] T. A. Beu, L. Horváth, and I. Ghişoiu, Phys. Rev. B **79**, 054112 (2009).
[9] H. Li, H. Tanga, and Y. Dou, Mol. Phys. **107**, 2039 (2009).
[10] A. Hussien, A. V. Yakubovich, A. V. Solov'yov, and W. Greiner, Eur. Phys. J. D **57**, 207 (2010).
[11] D. A. Papaconstantopoulos, M. J. Mehl, S. C. Erwin, and M. R. Pederson, in *Tight-Binding Approach to Computational Materials Science*, edited by P. E. A. Turchi, A. Gonis, and L. Colombo, MRS. Symposia Proceedings No. 491 (Materials Research Society, Pittsburgh, 1998), p. 221.
[12] T. A. Beu, J. Onoe, and K. Takeuchi, Eur. Phys. J. D **10**, 391 (2000).
[13] T. A. Beu, J. Onoe, and K. Takeuchi, Eur. Phys. J. D **17**, 205 (2001).
[14] T. A. Beu, J. Onoe, and A. Hida, Phys. Rev. B **72**, 155416 (2005).
[15] T. A. Beu and J. Onoe, Phys. Rev. B **74**, 195426 (2006).

[16]T. LeBrun, H. G. Berry, S. Cheng, R. W. Dunford, H. Esbensen, D. S. Gemmell, E. P. Kanter, and W. Bauer, Phys. Rev. Lett. **72**, 3965 (1994).
[17]T. Schlathölter, R. Hoekstra, and R. Morgenstern, J. Phys. B **31**, 1321 (1998).
[18]A. Itoh, H. Tsuchida, K. Miyabe, T. Majima, and Y. Nakai, Phys. Rev. A **64**, 032702 (2001).
[19]A. Itoh and H. Tsuchida, Nucl. Instrum. Methods Phys. Res. B **195**, 216 (2002).
[20]M. Tchaplyguine, K. Hoffmann, O. Duhr, H. Hohmann, G. Korn, H. Rottke, M. Wittmann, I. V. Hertel, and E. E. B. Campbell, J. Chem. Phys. **112**, 2781 (2000).
[21]B. Torralva, T. A. Niehaus, M. Elstner, S. Suhai, Th. Frauenheim, and R. E. Allen, Phys. Rev. B **64**, 153105 (2001).
[22]E. Kim, Y. H. Lee, and J. Y. Lee, Phys. Rev. B **48**, 18230 (1993).
[23]S. G. Kim and D. Tomanek, Phys. Rev. Lett. **72**, 2418 (1994).
[24]M. Boyle, T. Laarmann, I. Shchatsinin, C. P. Schulz, and I. V. Hertel, J. Chem. Phys. **122**, 181103 (2005).